IIETA International Information and Engineering Technology Association
Advancing the World of Information and Engineering

Journal of New Materials for Electrochemical Systems
Vol.22, No.3, July, 2019, pp. 132-138
http://new-mat.org
http://iieta.org/journals/jnmes

Sol-gel Synthesis and Characterization of $MgSO_4$:$Mg(NO_3)_2$ – Al_2O_3 Composite Solid Electrolytes

M. Sulaiman[1,*], N. Che Su[2] and N.S. Mohamed[3]

[1]Chemistry Division, Centre for Foundation Studies in Science, University of Malaya, 50603 Kuala Lumpur, Malaysia.
[2]Institute of Graduate Studies, University of Malaya, 50603 Kuala Lumpur, Malaysia.
[3]Physics Division, Centre for Foundation Studies in Science, University of Malaya, 50603 Kuala Lumpur, Malaysia.

Corresponding Author Email: mazdidas@um.edu.my

ABSTRACT

Composite solid electrolytes in the system (1-x)$MgSO_4$:$Mg(NO_3)_2$ – xAl_2O_3 with x = 0.1-0.6 were synthesized by sol- gel method and analysed by X-ray diffraction, differential scanning calorimetry, scanning electron microscopy, energy dispersive X-ray, Fourier transform infrared spectroscopy and alternating current impedance spectroscopy. Structural analysis revealed solid- solid phase transformation of anhydrous $MgSO_4$ to β - $MgSO_4$ after sintering at 900 °C for 2 hours. Recrystallization of crystalline β-$MgSO_4$ phase was observed for composite samples with x = 0.1 – 0.3. Addition of anhydrous $MgSO_4$ and $Mg(NO_3)_2$ as a co-host, resulted in the formation of MgO phase after heat treatment. The conductivities of the composites were in the order of 10-7 S cm^{-1} at room temperature on account from the formation of a new region of Mg_2+|MgO.

Keywords: *Magnesium sulphate, magnesium nitrate, composite solid electrolyte, XRD, DSC*

Received: June-17-2018, Accepted: January-20-2019, https://doi.org/10.14447/jnmes.v22i3.a03

1. INTRODUCTION

Currently, solid lithium ion electrolytes are the main materials used for Li^+ conduction by battery manufacturers. One such electrolyte used in solid batteries and available in the market is lithium iodide used for heart pace makers [1]. Solid electrolytes can be classified into various phases such as crystalline-polycrystalline, glassy-amorphous, composite and polymeric [2]. Composite solid electrolyte phase is the focus of our study. Composite solid electrolytes such as LiX – Al_2O_3 (X = Cl, Br, I) are the most fully studied [3 - 7] but these are although being toxic and expensive. An existing alternative for lithium is magnesium. Magnesium is environmentally friendly and non-toxic than lithium. Magnesium is chemically stable in oxygen atmosphere whilst helium or argon atmosphere is required when handling lithium metal. There is an urgent need for the development of magnesium electrodes and electrolytes with high energy density, thus applicable in solid-state electrochemical devices [8, 9]. Oddly enough, there is a dearth of information on magnesium composite solid electrolytes. In this case, to give a different perspective, we studied conductivity of composite solid electrolytes in the system of magnesium salts – oxide for future employment in magnesium-based rechargeable batteries.

We previously reported physical properties and conductivity mechanism of $Mg(NO_3)_2$ – Al_2O_3 composite solid electrolyte system [10]. It has been observed that the maximum value of ionic conductivity was found to be ~10^{-4} S cm^{-1} at room temperature. The enhancement of the conductivity was due to the formation of a new phase of magnesium oxide (MgO). We further study composite solid electrolytes in the system $MgSO_4$ – Al_2O_3 and $MgSO_4$:$Mg(NO_3)_2$ – MgO in order to develop suitable magnesium composite solid electrolytes [11,12]. In continuation, we further evaluate physical properties of MgSO4:$Mg(NO_3)_2$ – Al_2O_3 composite solid electrolytes in order to understand their ion transport capabilities. The effect of Al_2O_3 on ionic conductivity to the binary compound of magnesium sulfate ($MgSO_4$) and magnesium nitrate ($Mg(NO_3)_2$) was investigated.

Our results demonstrate that decomposition of $Mg(NO_3)_2$ and $MgSO_4$ salts lead to an increase in the ionic conductivity of the composite electrolytes.

The preparation route of the composite electrolytes was based on hydrolysis, condensation, gelling and drying of a solution containing magnesium sulphate, magnesium nitrate, alumina, ethanol and citric acid [13,14]. The composite electrolytes have been characterized using XRD, DSC, SEM, EDX, FTIR and impedance spectroscopic techniques.

2. EXPERIMENTAL

Composites with Al_2O_3 composition (mole) of x = 0.1 – 0.6 were prepared by sol-gel method. Anhydrous $MgSO_4$ (high purity grade), $Mg(NO_3)_2.6H_2O$ (high purity grade) and Al_2O_3 (high purity grade, particle size ~10 μm) were used as starting materials. The first step of the composite preparation was done by mixing the desired number of moles of magnesium sulphate, magnesium nitrate and alumina with ethanol under magnetic stirring at room temperature. The ratio of magnesium sulphate: magnesium nitrate was 2:1. An equal amount of citric acid to the mass of alumina was then added to the primary solution with continuous stirring for 20 min. Then, the solution was refluxed at 80 - 100 °C on a hot plate until the formation of a white gel. In the second step of the sol-gel process, white gel was kept in an oven at 200 °C until complete dryness. The final products obtained were voluminous, fluffy and white powders. The resulting mixtures were sintered at 900 °C for 2 h and quickly cooled. The precursor powders obtained were then ground in an agate mortar into fine powders. Structural characterizations for XRD and FTIR were performed on a D8 Advanced-Bruker X-ray Diffractometer with Cu Kα radiation and a Perkin Elmer Fron-

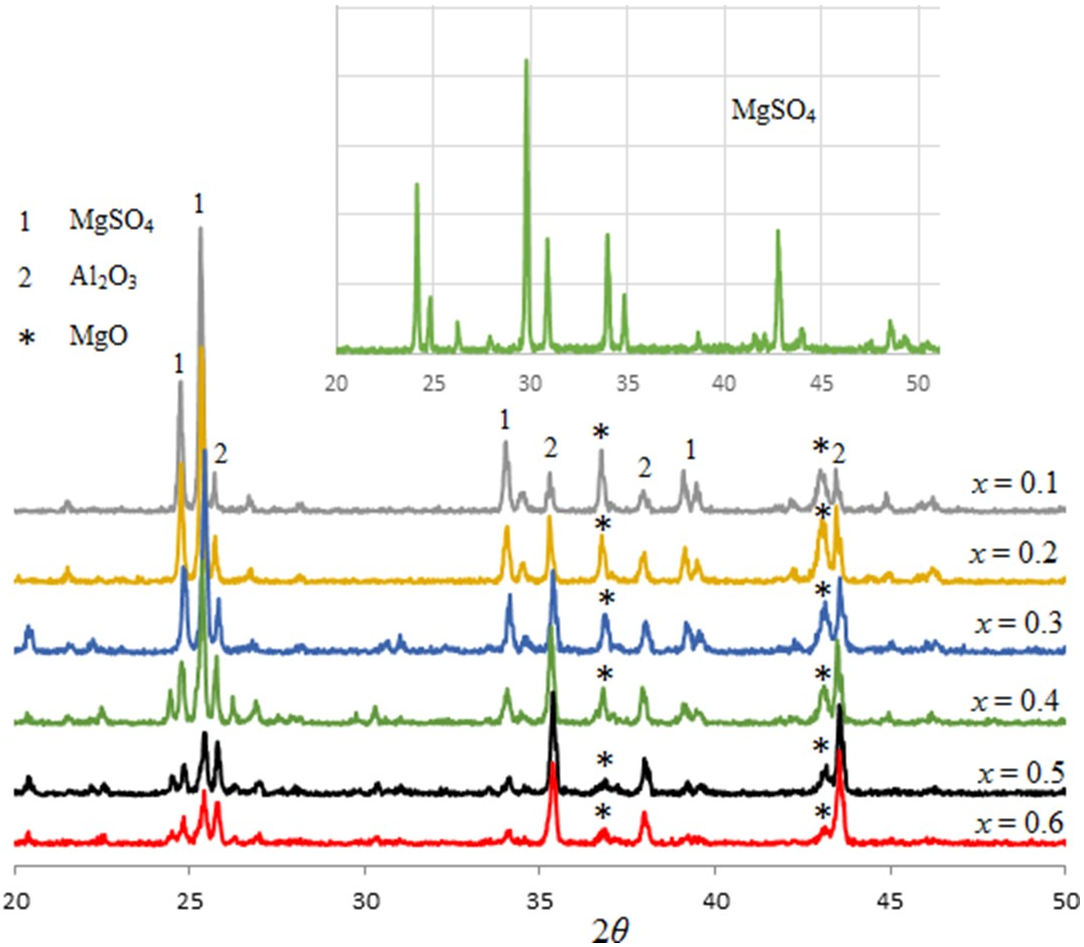

Fig. 1. XRD patterns of $MgSO_4$ and (1-x)$MgSO_4$:$Mg(NO_3)_2$ – xAl_2O_3 composites.

tier spectrometer, respectively. The thermal properties of the samples were measured on a Seteram Evo Labsys thermal analyser in a nitrogen atmosphere at a constant heating rate 5 °C min^{-1} at temperatures ranging from 30 to 1200 °C. The morphology and chemical content of the powders were analysed by SEM/EDX using Oxford Aztec X-act EDX spectrometer attached to a Zeiss-Evo MA10 Scanning Electron Microscope. For conductivity studies, pellets were made by pressing the composite powders at a pressure of 9-10 tones cm^{-2}. The diameter of the pellet was 13 mm and its thickness was about 1.1 mm. Conductivities were measured on a Solatron 1260 impedance analyser at temperatures ranging from room temperature to 150 °C by sandwiching composite pellet between two stainless steel electrodes. An ac amplitude of 200 mV in the frequency range of 10^{-1} – 107 Hz was used.

3. RESULTS AND DISCUSSION

3.1. XRD analysis

Fig. 1 provides X-ray diffraction pattern of MgSO4 and prepared composite samples with x = 0.1 – 0.6. Anhydrous MgSO4 showed predominant peaks at 2θ of ~25°, 30°, ~35° and 42.7°. Traces of other peaks were found very weak. In our sol-gel method, major changes of pattern are observed in composite samples with x = 0.1 - 0.6. Anhydrous $MgSO_4$ undergo a structural transformation to a crystalline β -$MgSO_4$ phase due to the heating effect on composite samples at 900 °C for 2 h [12]. From XRD diffraction pattern, all composite samples exhibited orthorhombic crystal structures of $\beta MgSO_4$ phase with

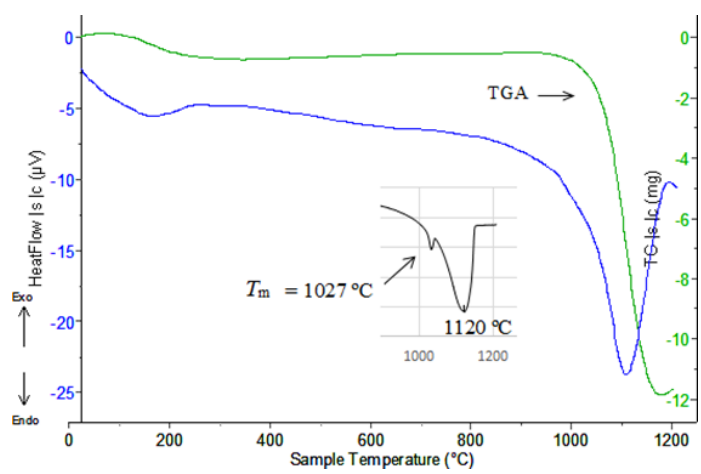

Fig. 2. DSC-TGA curves of $MgSO_4$

space groups of Pbnm62 [15-17]. The pattern obtained was in good agreement with standard β-$MgSO_4$ powder data (JCPDS 210546). Recrystallization of crystalline β-$MgSO_4$ phase was observed for composite samples with x = 0.1 – 0.3. At $x \geq 0.4$, a low crystallinity of β- $MgSO_4$ was observed at 2θ of 24.6° upon increasing the amount of alumina in the system. The broadening of peaks at 2θ = 34° and 39.5° indicated the formation of an amorphous phase of β- $MgSO_4$ in the

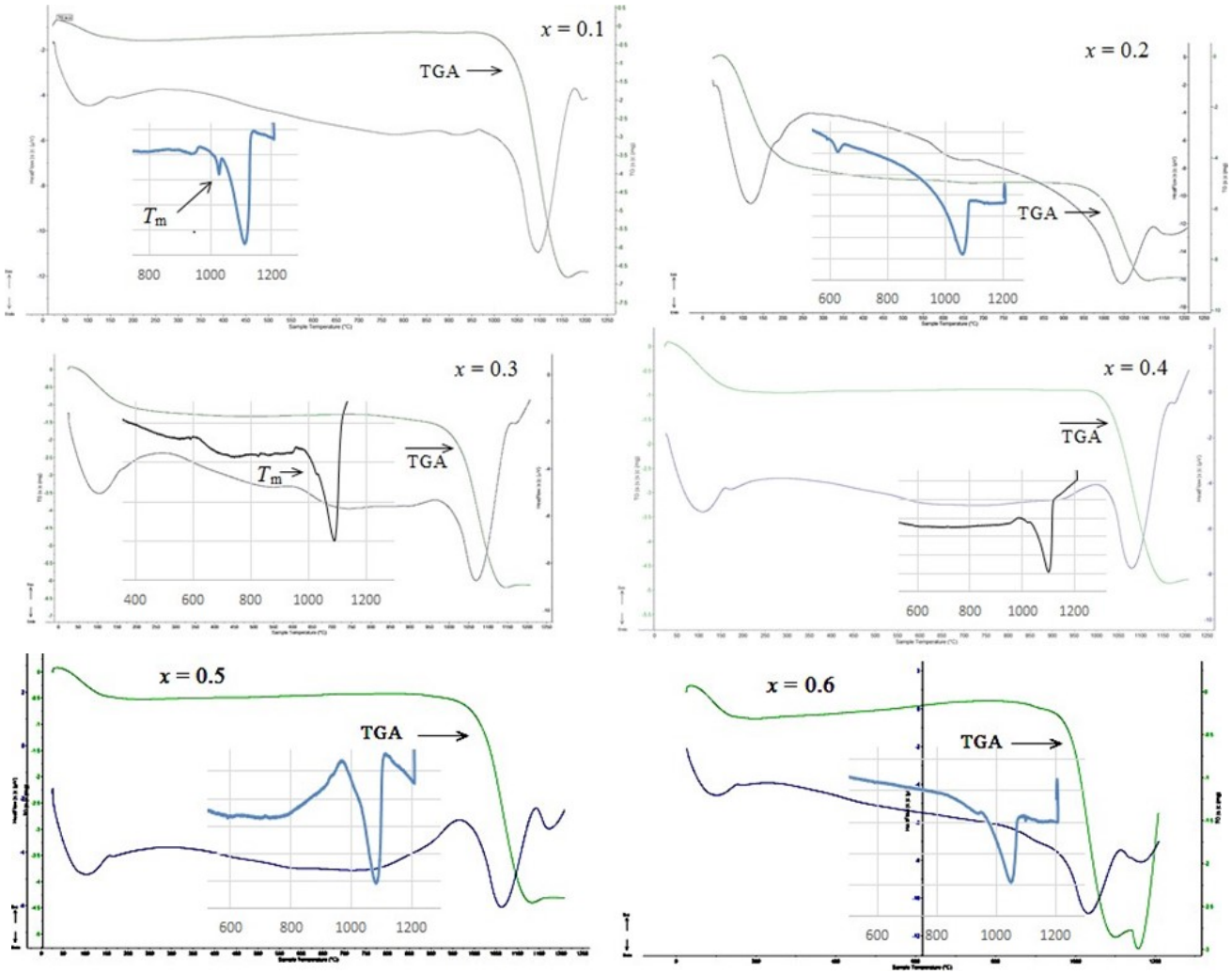

Fig. 3.1. DSC-TGA curves of (1-x)$MgSO_4$:$Mg(NO_3)_2$ – $x$$Al_2O_3$ composites

composite samples with x = 0.4 - 0.6. The formation of the phase was expected at β- $MgSO_4$ -Al_2O_3 interface as a result of chemical and physical interactions of both β-$MgSO_4$ and Al_2O_3 crystalline phases. In summary, the results of X-ray diffraction analysis showed that the composites obtained in this work exhibited two states of β -$MgSO_4$ phases: crystalline and amorphous. A possible pathway of structural transformation of magnesium sulphate in the mixture could be according to Eq. 1 [12, 15, 16]:

$$\begin{aligned} &\text{anhydrous } MgSO_4 \xrightarrow[< 900\ °C]{} \alpha\text{-}MgSO_4 \xrightarrow[900\ °C]{} \\ &\beta\text{-}MgSO_4 \longrightarrow \underset{\text{amorphous}}{\beta\text{-}MgSO_4} + \underset{\text{recrystallization}}{\beta\text{-}MgSO_4} \end{aligned} \quad (1)$$

Meanwhile, a new phase of MgO was formed in the composite samples prepared as indicated by peaks at 2θ = 37.0° and 43.1° as shown in Fig. 1 [8, 17]. Magnesium sulphate is reported to decompose into magnesium oxide when the temperature is 700 °C or higher [18, 19]. In this sol-gel method, decomposition of β-MgSO4 and $Mg(NO_3)_2.6H_2O$ phases yield an MgO product. The disappearance of $Mg(NO_3)_2.6H_2O$ peaks in all composite samples supported the formation of this new phase. Transformation route of crystalline $Mg(NO_3)_2.6H_2O$ is given in Eq. 2 and Eq. 3 [10, 20]:

$$Mg(NO_3)_2.6H_2O \rightarrow Mg(NO_3)_2 + 6H_2O \quad (2)$$

$$2Mg(NO_3)_2 \rightarrow 2MgO + 4NO_2 + O_2 \quad (3)$$

From the spectra, it is observed that the high-intensity diffraction peak at 2θ = 43.1° is associated with the high concentration of MgO phase in the composite sample with x = 0.2. This could be attributed to the limited amount of alumina particles present in the composite so that no blocking effect occurred for the transformation of phases of the crystalline. Consequently, low intensity of MgO peaks at x = 0.5 and 0.6, indicate that MgO exists as an amorphous phase in the composite samples.

The characteristic peaks of alumina are shown at 2θ of 25.3°, 35.3°, 37.8° and 43.4°. This confirms the composite nature of the samples. The intensity peaks of alumina are found to increase from x = 0.1 to 0.4 but decrease with further increase in x. This suggests amorphization of alumina particles in composite samples with x = 0.5 and 0.6. In summary, β-$MgSO_4$, MgO and Al_2O_3 phases coexist in all the composite samples (x = 0.1 – 0.6).

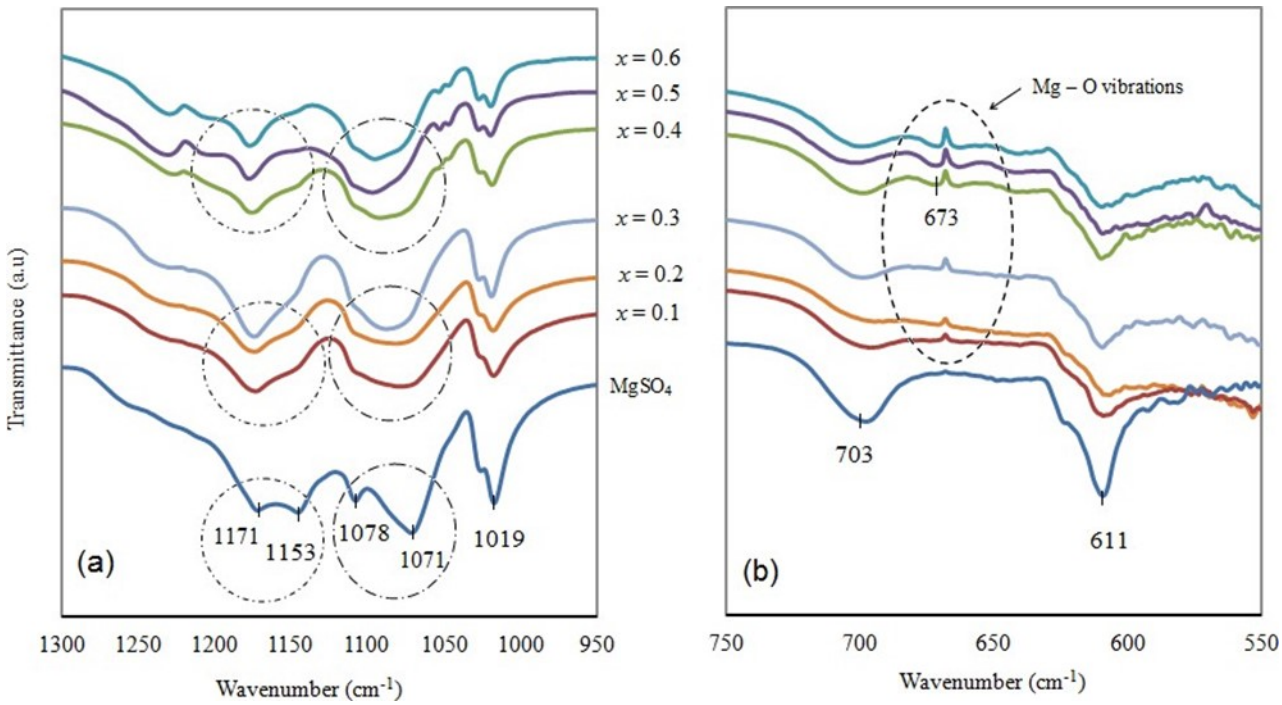

Fig. 3.2. FTIR spectra of $MgSO_4$ and (1-x)$MgSO_4$:$Mg(NO_3)_2$-xAl_2O_3 composites from (a) 950 to 1300 cm^{-1} and (b) 550 to 750 cm^{-1}.

3.2. DSC and TGA analyses

Coupled DSC – TGA curve of $MgSO_4$ is shown in Fig. 2. Two endothermic peaks at 1027 °C and 1120 °C are attributed to melting (Tm) and decomposition of $MgSO_4$, respectively [12, 19 - 22]. The melting (Tm) and decomposition behaviour of the prepared composite samples (x = 0.1 – 0.6) are shown in Fig. 3. In these composite samples, the shift of the melting points (Tm) at ~940 – 1022 °C is due to the presence of alumina particles. There is no melting point of crystalline $MgSO_4$ at $x \geq 0.4$. This phenomenon could be attributed to the phase change of crystalline $MgSO_4$ to the amorphous phase in the composite samples with x = 0.4 – 0.6. The low-crystallinity of β - $MgSO_4$ in the composite samples is indicated by the XRD result as shown in Fig.1.

The amorphization of β - $MgSO_4$ salt is expected to occur as x increases (high alumina concentration). The spreading of β - $MgSO_4$ salt over the alumina particles yield the amorphous phase of β - $MgSO_4$. The ionic salt is likely to spread only in a molten state, which is closed to Tm.

At x = 0.2, a small endothermic peak at 628 °C could be attributed to a phase transition from an amorphous $MgSO_4$ to semi-crystalline MgO as shown by the XRD spectrum [20, 21]. The decomposition of β - $MgSO_4$ phase can be represented by the following route [18, 19]:

$$\beta\text{ - } MgSO_4 \rightarrow MgO\ (s) + SO_3 \qquad (4)$$

3.3. FTIR analysis

The FTIR spectra of $MgSO_4$ and composite samples with x = 0.1 - 0.6 are presented Fig. 3. All spectra showed characteristic sulphate group peaks at 611, 703, 1019, 1071 - 1078 and 1153 - 1171 cm^{-1} demonstrating the presence of $MgSO_4$ phases in composite mixtures [15,16]. A sharp band at 611 cm^{-1} was assigned to the bending mode of S – O bonds. For composite samples with x = 0.3 – 0.6, the broad absorption band at 612 cm^{-1} probably resulted from the combined absorptions of sulphate and other vibrations of alumina or MgO molecules indicating disordered sulphate ions in $MgSO_4$ [23]. The splitting of the sulphur - oxygen stretch at 1071 - 1078 and 1153 - 1171 cm^{-1} was not observed in the spectra of the composite samples with x = 0.1 to x = 0.6. This observation suggests the change of crystalline structure of anhydrous $MgSO_4$ to β - MgSO4 phase, as supported by XRD analysis. The synthesis of composite solid electrolytes in the system (1- x)$MgSO_4$:$Mg(NO_3)_2$ – xAl_2O_3 allowed the formation of MgO phases in all composite samples (x = 0.1 - 0.6) as evidenced firstly by disappearance of band absorptions of nitrate group in all composite samples and secondly with appearance of bands at 673 cm^{-1} which could be assigned to Mg – O vibrations [10,17, 23, 25]. The intensity of the band increased from x = 0.1 to x = 0.6 demonstrating an increase in concentration of MgO phases.

3.4. SEM/EDX analysis

Fig. 4 shows SEM micrographs of composite samples with x = 0.2 and x = 0.5. For both composite samples, the image could be translated as spreading of β - $MgSO_4$ phase (white) over the alumina grains. At x = 0.2, magnesium sulphate was partially transformed into an amorphous state of β - $MgSO_4$ as indicated by the XRD analysis. The spreading of melted magnesium sulphate on alumina grains led to the formation of an amorphous phase of β - $MgSO_4$ during the sintering process [26 - 28]. At this composition, the particle sizes of β - $MgSO_4$ were between ~200 nm to micro scale level. The interaction between magnesium salts of nitrate and sulphate, with dispersoid of alumina grains, favoured the formation of MgO phase near to magnesium salt/dispersoid interface. Some dark areas that could be attributed to the amorphous phase of MgO, showed good inter-phase contact with β - $MgSO_4$ amorphous phase. Fig. 5 shows EDX spectra elucidating the chemical composition of the composite sample with x = 0.5. The presence of Mg, Al, S and O elements could be attributed to $MgSO_4$, MgO and Al_2O_3 as previously suggested by XRD results.

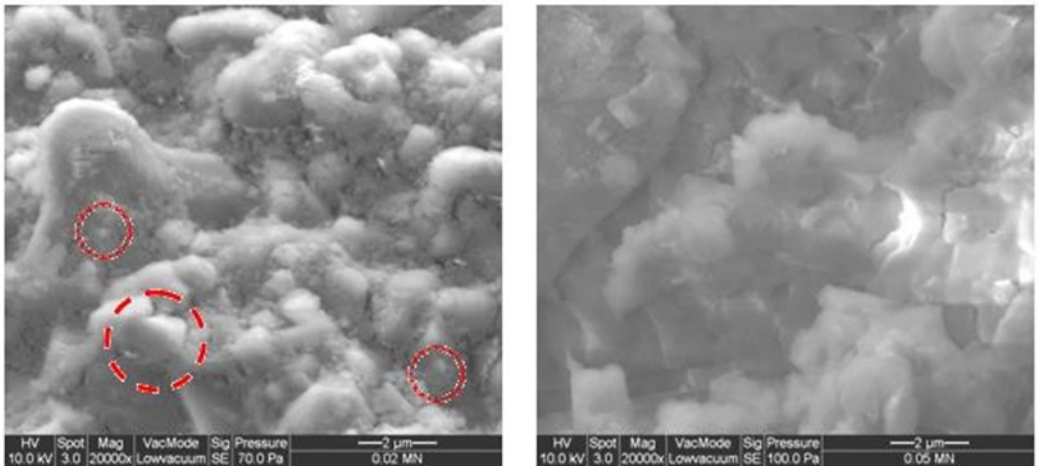

Fig. 4. Morphology of composite samples with (a)x=0.2 and (b)x=0.5 magnified at 20000 x represents nanosaized particles and represents the micro sized particles.)

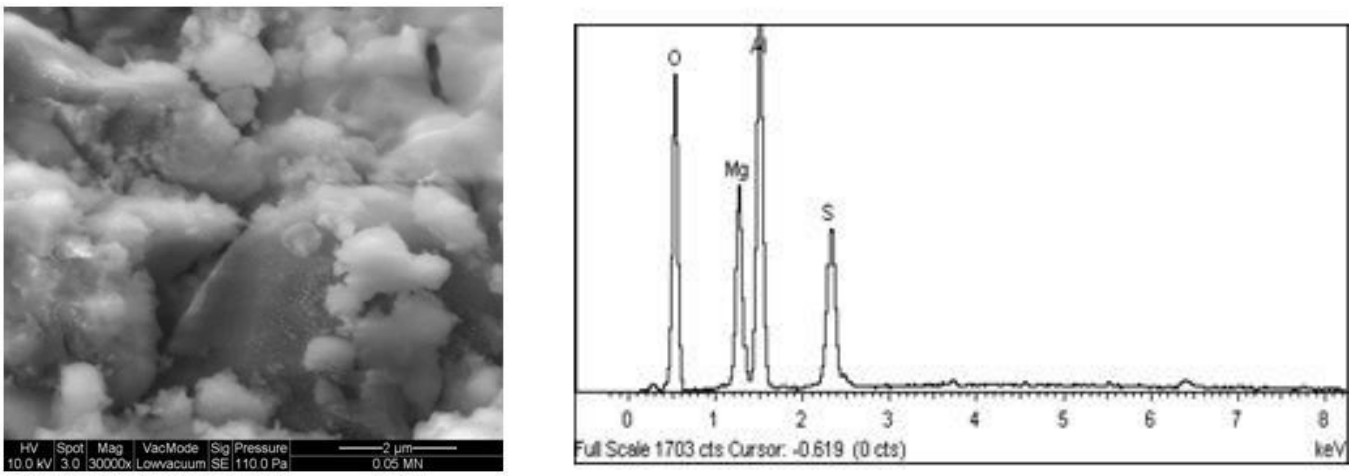

Fig. 5. SEM/EDX spectra for composite sample with x = 0.5.

3.5. Ionic conductivity

Complex impedance plots of composite samples with x = 0.1 - 0.6 at room temperature (30 °C) are shown in Fig. 6. The spectra consist of a semicircle at higher frequency followed by a spike at a low-frequency region. The semicircle with the interception at the Z'-axis was assigned to bulk resistance (*Rb*). The formation of spike represented interfacial effects between electrode and electrolyte [23, 24]. The equivalent circuit of composite samples determined from complex impedance plot (Fig. 6) comprised of bulk resistance Rb, bulk capacitance Cb (CPE) and CPE blocking electrode with a constant phase element (CPE) behaviour. In the present work, by knowing the value of bulk resistance (*Rb*), the conductivity was calculated using the relationship as shown below:

$$\sigma_b = d\, R_b\, A \qquad (5)$$

where d is the sample thickness (cm), *Rb* is bulk resistance (W), and A is the area (cm^2) of the sample.

Fig. 7 represents the conductivity behaviour at room temperature (30 °C) of composite samples with different Al_2O_3 particles composition (x). From the plot, two conductivity maxima were observed at

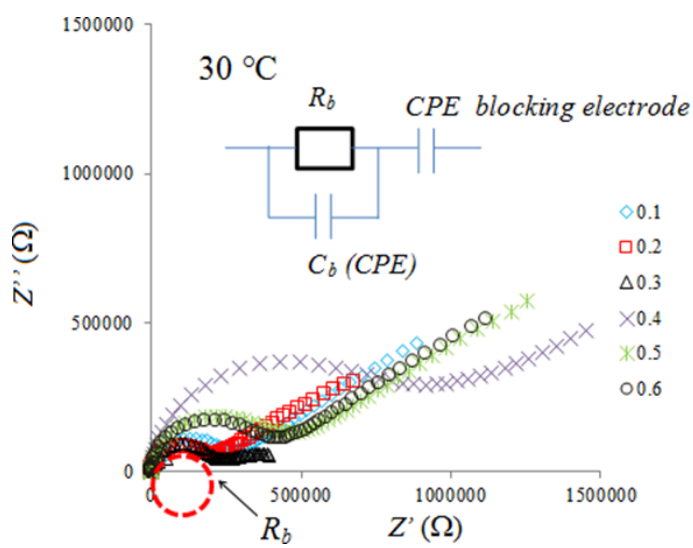

Fig. 6. Complex impedance spectra of (1-x)$MgSO_4$:$Mg(NO_3)_2$ – $x$$Al_2O_3$ composites.

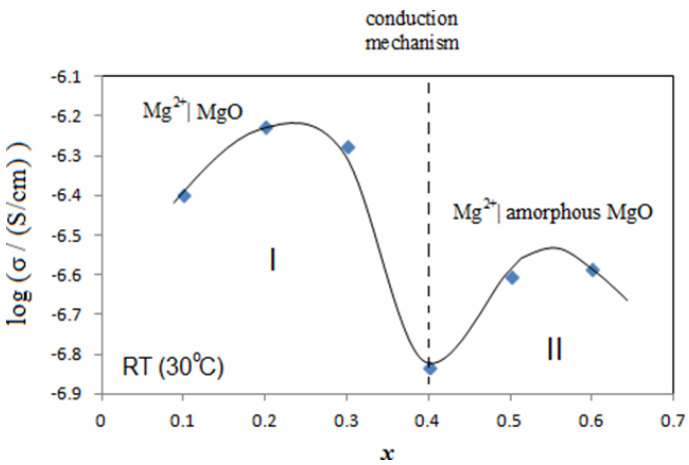

Fig. 7. The ionic conductivity as a function of composition (x) for (1-x)$MgSO_4$:$Mg(NO_3)_2$ - xAl_2O_3 at room temperature.

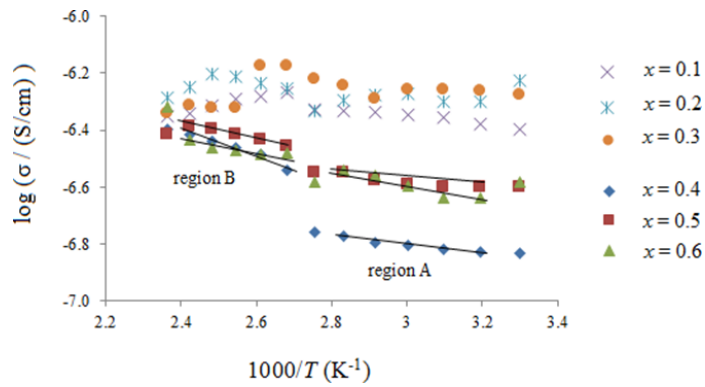

Fig. 8. The ionic conductivity of composites (1-x)$MgSO_4$:$Mg(NO_3)_2$ - xAl_2O_3 versus the inverse of temperature at various compositions.

x = 0.2 and x = 0.5 – 0.6 providing evidence for two different conductivity mechanisms in the system. For the first part of the plot (region I), the ionic conductivity from x = 0.1 to x = 0.3, could be explained by the spreading of recrystallized $MgSO_4$ salt over the surface of MgO. The adsorption of Mg^{2+} cations on the oxide surface ($MgSO_4$|MgO) can be explained by a chemical interaction between Lewis acid of Mg^{2+} cations from β - $MgSO_4$ and Lewis base of MgO phase [3, 28]. The formation of a new region of $MgSO_4$|MgO interface, increased the mobility of Mg^{2+} cations in the composites [28]. The decrease in conductivity beyond x = 0.3 could be interpreted by agglomeration of alumina particles hampering the migration of charge carriers in the samples [13,29].

As for the second part of the plot (region II), the transformation of crystalline $Mg(NO_3)_2.6H_2O$ into MgO amorphous phase explain a sharp increase of conductivity from x = 0.4 to 0.5. Association between Mg^{2+} cations from amorphous phase of β - MgSO4 and appearing MgO phase evoked the formation of amorphous-MgO|Mg^{2+} interfaces facilitating the mobility of Mg^{2+} cations and thus the conductivity of composite samples [8 - 10]. As revealed by XRD, FTIR and SEM, increased in concentrations of both MgO and β - $MgSO_4$ amorphous phases from x = 0.4 – 0.6 imposed a clear increased in Mg^{2+} cations mobility and consequently, conductivity. This phenomenon corroborates our previous ionic conductivity analysis using $Mg(NO_3)_2$ - Al_2O_3 system [10].

Fig. 8 shows the temperature dependence of conductivity for composite samples in the system (1- x)MgSO4:$Mg(NO_3)_2$ - xAl_2O_3. The conductivities of samples increased with increasing temperature. Two conductivity changes occurred in the system at a temperature range from 30 to 90 °C (region A) and from 100 to 150°C (region B) implying two phase changes as the temperature increase. The temperature dependence of ionic conductivity is given by the Arrhenius equation as

Table 1. Room temperature values of ionic conductivity and activation

Composite samples	σ (S cm^{-1})	*Ea* (eV)	
		40 – 80 °C	100 – 150 °C
x = 0.4	1.48 × 10-07	0.9374	0.9689
x = 0.5	2.50 × 10-07	0.8270	0.6240
x = 0.6	2.61 × 10-07	0.9385	0.6074

$$\log \sigma = \log \sigma_{\circ} - Ea\ /kT \tag{6}$$

where $\sigma_{\circ}$ is the pre-exponential factor, k is Boltzmann constant and *Ea* is the activation energy which can be computed by the least square linear fitting of log σ – 1/T plots. For composite samples with x = 0.1 – 0.3, conductivities were owed to the presence of partially amorphous phase of β - $MgSO_4$. This is consistent with the non-linear Arrhenius plot in Fig. 8 [13]. On the other hand, the conductivities of composite samples with x = 0.4 – 0.6 were stable probably due to the predominance of amorphous state of β - $MgSO_4$. For composite samples with x = 0.4 – 0.6, the values of *Ea* obtained are tabulated Table 1.

A decrease in *Ea* from region A to region B is attributed to the semi-crystalline– amorphous transition phase of β - $MgSO_4$. At x = 0.5 – 0.6, β - $MgSO_4$ has complete amorphous phase. Overall, the low conductivity values of composite solid electrolytes in the system (1-x)$MgSO_4$: $Mg(NO_3)_2$ — xAl_2O_3 repose on strong electrostatic forces between the Mg^{2+} and SO^{2-} ions which hamper the mobility of Mg^{2+} ions in composite samples.

4. CONCLUSION

Composite solid electrolytes in the system (1-x)$MgSO_4$:$Mg(NO_3)_2$ – xAl_2O_3 were synthesized using a sol-gel technique. The XRD analysis revealed the presence of both crystalline and amorphous states of β - $MgSO_4$. Structural analysis showed a formation of MgO phase due to $Mg(NO_3)_2.6H_2O$ and $MgSO_4$ phase transitions, in all composite samples. The composite system exhibited two types of conductivity mechanisms based on Mg^{2+}|MgO interfaces for composite samples with x = 0.1 – 0.3 and via Mg^{2+}|amorphous-MgO interfaces for composite samples with x = 0.4 – 0.6. Low conductivity values of composite solid electrolytes in the system (1-x)$MgSO_4$:$Mg(NO_3)_2$ - xAl_2O_3 resulted from strong electrostatic forces between the Mg^{2+} and SO_4^{2-} ions. The present results warrant further evaluation of magnesium salts composite solid electrolytes at room temperature for the development of magnesium salt based batteries.

5. ACKNOWLEDGEMENT

The authors would like to thank the University of Malaya for granting the Research Grant (RG254/13AFR) to support this work.

REFERENCES

[1] Holmes CF, Electrochem. Soc. Interface, 26 (2003).
[2] Agrawal RC, Gupta RK, J. Mater. Sci., 34, 1131 (1999).

[3] Ulihin AS, Uvarov NF, Russ, J. Electrochem., 45, 707 (2009).
[4] Liang CC, J. Electrochem. Soc., 120, 1289 (1973).
[5] Poulsen FW, Andersen, NH, Kindl B, Schoonman, J. Solid State Ionics, 9-10, 119 (1983).
[6] Uvarov NF, Bokhonov BB, Isupov VP, Hairetdinov EF, Solid State Ionics, 74, 15 (1994).
[7] Chen L, Zhao Z, Wang C, Li Z, Acta Phys. Sin., 34, 1027 (1985).
[8] Pandey GP, Agrawal RC, Hashmi SA, J. Power Sources, 190, 563 (2009).
[9] Pandey GP, Agrawal RC, Hashmi SA, J. Phys. Chem. Solids, 72, 1408 (2011).
[10]Sulaiman M, Rahman AA, Mohamed NS, Int. J. Electrochem. Sci., 8, 6647 (2013).
[11]Sulaiman M, Che Su N, Mohamed NS, J. New Mat. Electrochem. Systems, 19, 27 (2016).
[12]Sulaiman M, Che Su N, Mohamed NS, Ionics, 23, 443 (2017).
[13]Sulaiman M, Dzulkarnain NA, Rahman AA, Mohamed NS, Solid State Sci., 14, 127 (2012).
[14]Li Y, Wang Q, Yang H, Curr. Appl. Phys., 9, 1375 (2009).
[15]Smith DH, Seshadri KS, Spectrochim. Acta A., 55, 795 (1999).
[16]Manam J, Das S, Solid State Sci., 12, 1435 (2010).
[17]Tamilselvi P, Yelilarasi A, Muthusamy Hema M, Anbarasan R, Nano Bulletin, 2, 1301061 (2013).
[18]Scheidema MN, Taskinen P, Ind. Eng. Chem. Res., 50, 9550 (2011).
[19]L'vov BV, Ugolkov VL, Thermochim. Acta., 411, 73 (2004).
[20]Bokhimi, Morales A, Lopez T, Gomez R, J. Solid State Chem., 115, 411 (1995).
[21]Pop SF, Ion RM, J. Optoelectron Adv. M., 15, 888 (2013).
[22]Torres J, Mendez J, Sukiennik M, Thermochim. Acta, 334, 57 (1999).